An Augmented Reality System for Epidural Anesthesia (AREA): Prepuncture Identification of Vertebrae

Hussam Al-Deen Ashab, Victoria A. Lessoway, Siavash Khallaghi, Alexis Cheng, Robert Rohling, and Purang Abolmaesumi*

***Abstract*—We propose an augmented reality system to identify lumbar vertebral levels to assist in spinal needle insertion for epidural anesthesia. These procedures require careful placement of a needle to ensure effective delivery of anesthetics and to avoid damaging sensitive tissue such as nerves. In this system, a trinocular camera tracks an ultrasound transducer during the acquisition of a sequence of B-mode images. The system generates an ultrasound panorama image of the lumbar spine, automatically identifies the lumbar levels in the panorama image, and overlays the identified levels on a live camera view of the patient's back. Validation is performed to test the accuracy of panorama generation, lumbar level identification, overall system accuracy, and the effect of changes in the curvature of the spine during the examination. The results from 17 subjects demonstrate the feasibility and capability of achieving an error within clinically acceptable range for epidural anaesthesia.**

***Index Terms*—Augmented reality, epidural anesthesia, image guidance, interventional ultrasound, panorama ultrasound.**

I. Introduction

EPIDURAL anesthesia is an injection of local anesthetics and antiinflammatory medication into the epidural space near the spinal canal for pain management. Injection into the lumbar region at the L2-L3 or L3-L4 is commonly used in obstetrics for pain relief of labor and delivery. Epidural anesthesia can also be used as an alternative to general anesthesia [1]. To effectively deliver anesthetics and/or antiinflammatory medication, a two-step procedure has to be successfully performed. The puncture site should be correctly selected at the desired intervertebral space followed by appropriate selection of needle trajectory to reach the target. Both of these steps are currently done blindly with manual palpation. Identification of the vertebrae for the first step is only 30% accurate [2]. Therefore, 70% of the procedures misidentify the desired intervertebral space by one or more levels. This is undesirable for two reasons. First, accidental needle overshoot is more likely to result in nerve damage for higher vertebrae. Second, the effectiveness of the anesthetics depends on the level [2].

Recent studies have shown that ultrasound can be used to accurately identify the vertebral levels [3]–[6]. However, interpreting spinal ultrasound images remain a challenge, especially for novice ultrasound operators (i.e., many anesthesiologists).

To alleviate this issue, our research team has previously proposed two techniques for automatic vertebral levels identification from panorama ultrasound images [7] and displaying the level to the anesthesiologist in an ultrasound guidance system with a camera mounted on the transducer [8]. However, there are remaining challenges that need to be addressed to enable the translation of ultrasound-guided epidural anesthesia in routine clinical practice: 1) A system has to be developed to seamlessly relate the identified vertebral levels to the patient's skin while accommodating some patient motion during the epidural procedure; and 2) there should be no disruption to the sterile field such as modifying the ultrasound transducer by mounting a camera system, as previously proposed [8].

This research makes two major contributions. First, a new, efficient, and fully automatic lumbar level identification algorithm from panorama ultrasound images is developed. Second, it proposes an augmented reality system for Epidural anesthesia (hereafter referred to as AREA) that overlays the identified levels on a live video image of the patient's back. The workflow of AREA is as follows. 1) Initially, a sequence of ultrasound images is acquired from the patient's back before needle insertion. These images are used to generate a panorama image showing a sagittal cross section of the spinal anatomy parallel to the main spinal axis. 2) An automatic image processing technique identifies the lumbar levels in the panorama image. 3) An augmented reality module converts the level location in the panorama image relative to the camera's view of the patient, and overlays virtual markings of the levels on a live video display of the patient's back.

This workflow ensures minimum disruption in the current clinical procedure. Furthermore, since a remote video camera

Manuscript received February 5, 2013; revised March 15, 2013; accepted April 20, 2013. Date of publication May 13, 2013; date of current version August 16, 2013. *Asterisk indicates corresponding author.*

H. Al-Deen Ashab and S. Khallaghi are with the Department of Electrical and Computer Engineering, University of British Columbia, Vancouver, BC V6T 1Z4, Canada (e-mail: hussama@ece.ubc.ca; siavashk@ece.ubc.ca).

V. A. Lessoway is with the British Columbia Women's Hospital and Health Centre, Department of Ultrasound, Vancouver, BC V6H 3V4, Canada (e-mail: vickie@lessoway.ca).

A. Cheng is with the Department of Computer Science, Johns Hopkins University, Baltimore, MD 21218 USA (e-mail: acheng27@jhu.edu).

R. Rohling is with the Department of Electrical and Computer Engineering, Department of Mechanical Engineering, University of British Columbia, Vancouver, BC V6T 1Z4, Canada (e-mail: rohling@ece.ubc.ca).

*P. Abolmaesumi is with the Department of Electrical and Computer Engineering, University of British Columbia, Vancouver, BC V6T 1Z4, Canada (e-mail: purang@ece.ubc.ca).

Color versions of one or more of the figures in this paper are available online at http://ieeexplore.ieee.org.

Digital Object Identifier 10.1109/TBME.2013.2262279

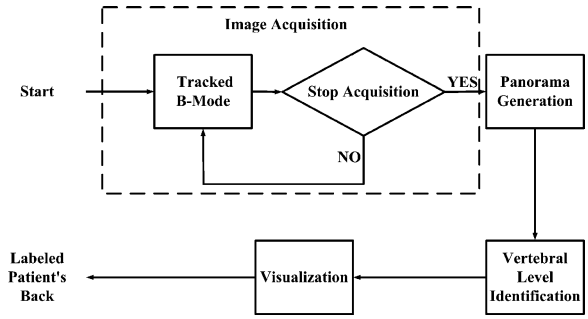

Fig. 1. Workflow of AREA.

is used, the system does not interfere with the sterile field. The original design and preliminary results on ten human subjects have been reported previously [9]. This paper provides substantially more detail on the description and implementation of the technique, and reports extensive validation of the system for 17 subjects. It also compares the performance of vertebral levels identification technique we propose with a competing method previously reported by Kerby *et al.* [7]. The paper is organized as follows: Section II describes the materials and methods used in identifying the lumbar level. In particular, it includes 1) panorama image generation, 2) vertebral levels identification, and 3) visualization. Section III describes the experiments and results. Section IV provides a discussion, concluding remarks, and future work.

II. Materials and Methods

AREA consists of a SonixTOUCH ultrasound system (Ultrasonix Medical Corp., Richmond, Canada) equipped with a 6.6-MHz linear array transducer, L14-5/38; imaging parameters: depth 6.0 cm, dynamic range 56 dB, gain 50%, and 16 frames per second) and a trinocular MicronTracker motion tracking system (Claron Technology Inc., Toronto, ON, Canada) to track two markers. The first one is placed on the transducer so it is referred to as the "Transducer Marker." The second marker is affixed to the patient's back approximately 50 mm lateral to L3, which is close to the approximate puncture site, but outside the sterilized area, and referred to as the "Patient Marker."

A simplified workflow of spinal needle insertion with guidance from AREA is shown in Fig. 1. First, the system checks if all markers are visible followed by a prompt for the sonographer to start. The transducer is initially placed in the parasagittal plane, 10 mm away from the midline on the interspinous gap L5-S1. As shown in Fig. 2, the sonographer moves the transducer superiorly across the lamina from the interspinous gap L5-S1 to the interspinous gap T12-L1 to acquire the set of images.[1]

Each image is recorded individually by pressing a foot pedal. During the scan, the sonographer determines the suitability of each image for the subsequent steps, if the image contains:

1) a wave-like pattern from the laminae surfaces;

[1]N.B. the sonographer also used a curvilinear transducer (C5-2, Ultrasonix Medical Corp., Richmond, Canada), which was capable of displaying two to three vertebral lamina in a single ultrasound image. These images were used to measure the vertebral height for the purpose of validation as described in detail in Section III.

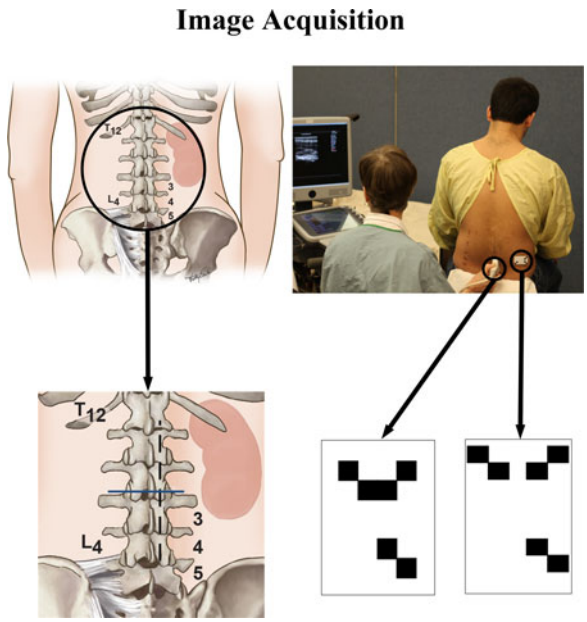

Fig. 2. Ultrasound B-mode images are acquired by placing the transducer in the parasagittal plane 10 mm from the midline. The solid line shows the vertebral level the system identifies and the dashed line shows the imaging plane acquired by the sonographer.

2) bright echoes from the most superior surface of the laminae;
3) distinct shadows under the laminae;
4) 50–70% overlap with the previous image.

These criteria ensure that adjacent images contain similar anatomical features that allow interslice registration when generating the panorama of the lumbar spine. Moreover, the 50–75% overlap between images is a compromise between the accuracy of registration (large overlap) and speed of examination (small overlap).

A. Panorama Generation

The position and orientation of the ultrasound images must be known for AREA to identify and display the lumbar levels accurately. Therefore, the N-wire calibration method integrated within an open-source software library for ultrasound imaging research (PLUS) [10] was used to calibrate the ultrasound image to the marker on the transducer. Using this calibrated transducer, a sequence of B-mode ultrasound images is acquired while tracked by the MicronTracker in the camera coordinate system. The stitching process then uses the estimated transformation between images from the tracker and a subsequent rigid registration using the Insight Toolkit [11] to automatically register and create a panorama ultrasound image of consecutive vertebrae B-mode images. To allow a smaller search space for the alignment parameters and less likelihood of large misregistration errors, the tracking information provided by the MicronTracker is used as an initial guess for the feature alignment followed by a standard normalized cross correlation with gradient descent optimizer, linear interpolation of image intensities at a noninteger pixel position, and translation transformation for the final alignment. Even though the MicronTracker has high

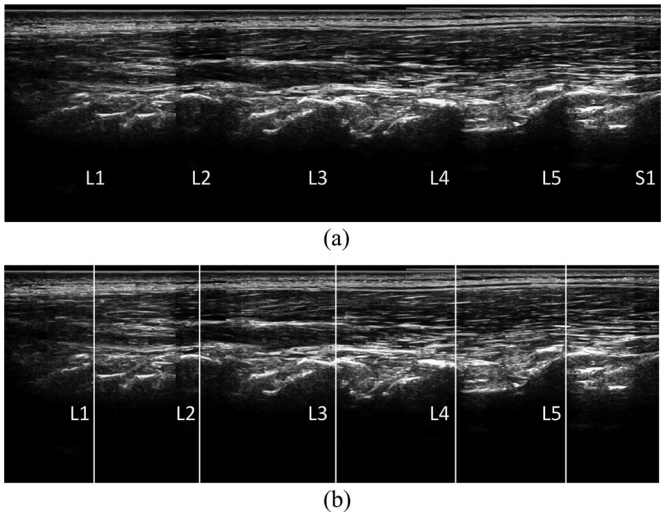

Fig. 3. Example of two ultrasound panorama images. (a) Panorama obtained in the parasagittal plane, showing L1, L2, L3, L4, L5, and S1 from left to right. (b) The same panorama image showing the automatically identified levels L1, L2, L3, L4, and L5 from left to right.

reported accuracy (marker tracking error of about 0.20 mm), it is sensitive to illumination conditions, specular reflections, and the orientation of a tracked tool, which affects the accuracy of tracking of individual ultrasound frames. These problems were also reported in a previous study by Maier-Hein *et al.* [12]. Therefore, to improve robustness in a clinical environment, we used an optimization and image registration algorithm to refine the tracking measurements. We used a gradient descent optimizer with normalized cross correlation as the image similarity measure. Our experience with the system in preliminary testing suggested that the choice of the optimizer and similarity measure did not affect the registration outcome. However, omitting the image registration step resulted in small but observable misalignments of the sequential ultrasound images.

This registration technique may still be susceptible to errors associated with accidental out-of-plane motions of the transducer, but with reasonable care during scanning, it generates panorama images sufficient for the purpose of vertebral levels identification. An example of panorama image is shown in Fig. 3. If the operator is unsatisfied with the quality of the panorama, a new panorama can be generated since a panorama can be acquired in less than 2 min. This primarily includes the time the operator takes to find the proper imaging plane, as it may be challenging in some cases to find a plane that clearly displays the epidural space. The actual panorama generation process, after acquiring all the ultrasound images, takes in the order of seconds. After the panorama image is generated, an automatic image processing technique identifies the lumbar levels. An identification example is shown in Fig. 3.

B. Vertebral Levels Identification

The challenge of identifying the lumbar levels arises from speckle, low contrast, and shadowing in the ultrasound images. These challenges come from the complex shape of the vertebrae and the presence of multiple ligaments, muscle, and fat, all of which generate echoes dependent on the angle of incidence of the ultrasound beam. Therefore, several processing steps are required for successful vertebral identification.

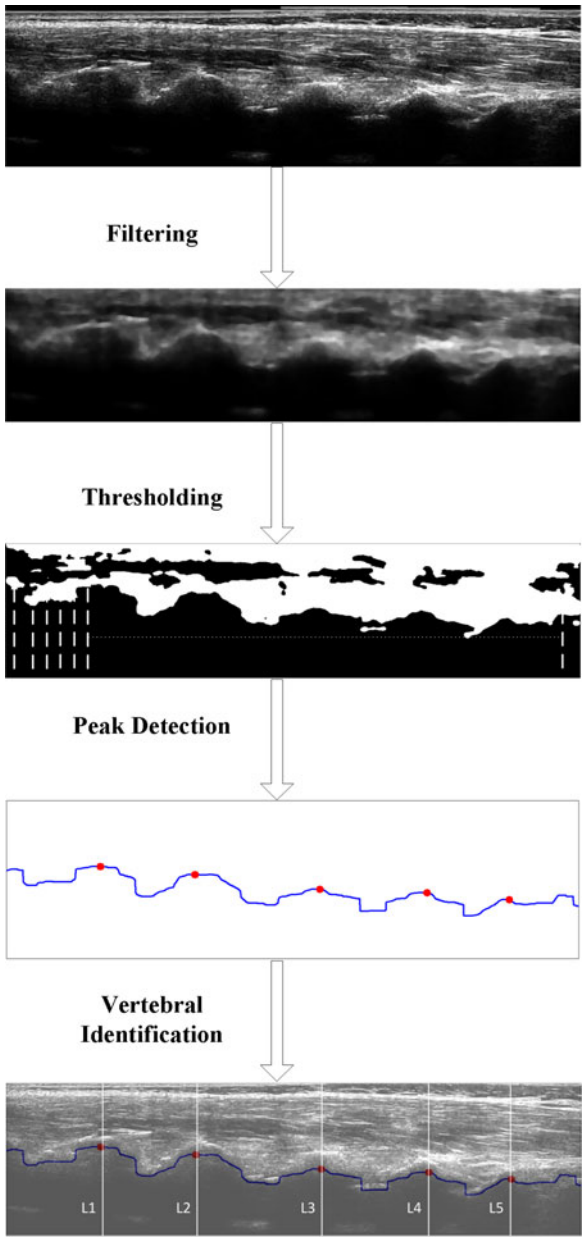

Fig. 4. Workflow of panorama image processing, thresholding, and vertebral identification, with the final step showing the fusion of the identification results with the original panorama image.

Filtering starts with a median filter over a window twice the size of a resolution cell, which corresponds to the smallest resolvable detail. After that, a bilateral filter [13], which smoothens images while preserving edges, is used to reduce the interclass variance and maximize the outer class variance. The closeness and similarity functions of the bilateral filter are both Gaussian functions. We set the size of the filter window to 40 pixels and the spatial-domain standard deviation is chosen as 5 pixels. The intensity-domain standard deviation depends on the standard deviation of image intensities. Fig. 4 shows an example of the filtering.

Ultrasound echoes are stronger from specular reflections, such as bony surfaces, than they are from soft tissues. This suggests a simple thresholding may be sufficient to separate the bone surface from tissue. However, previous research [14], [15] reports the difficulty of segmenting bone and tissue in ultrasound images with such simple thresholding. In AREA, we take advantage of the unique signature of the vertebral images in the ultrasound data (i.e., the shadow that appears under the lamina), and aim to segment this signature from the panorama images. Given the variable overall image intensity variations inherent between the ultrasound images from different subjects, we use an automatic thresholding technique based on Otsu's method [16]. This method assumes the image contains two classes of pixels: foreground (i.e., the soft tissue and lamina) and background (i.e., the shadow underneath each lamina). Under this assumption, this method calculates the optimum threshold separating those two classes so that intraclass variances are minimal.

The laminae in the lumbar spine appears as wave-like patterns in the panorama image. This signature is used to convert the 2-D panorama image to a 1-D signal. After thresholding the ultrasound panorama image, it is scanned along the echo direction from the bottom of the image to the top of the image. Whenever a value above Otsu's threshold value from the previous step is reached, the index value is used as a sampled point in the 1-D signal as shown in Fig. 4. Then, a median filter is applied to the signal followed by a peak detection technique to identify the peaks in the signal. The peak detection technique starts from left to right of the image, and when it detects a maximum followed by a minimum, it assigns a peak label. For each of the peaks, a threshold equal to the height of the vertebrae is used to remove any false peaks. Next, the thresholded peaks are considered as the middle sections of the laminae in the panorama ultrasound image as shown in Fig. 4. Given that the scanning starts at L5-S1, the vertebrae are labeled sequentially from L1 to L5.

C. Visualization

The MicronTracker is calibrated to extract coefficients of projection ray equations that convert pixel locations in an image into projection rays in the camera coordinate system. In the camera Software Development Kit (SDK) (Claron Technology Inc., Toronto, ON, Canada), the back projection ray is represented by a point in space and its angular orientation from the image axes. The projection equation coefficients are found by presenting to the camera a 3-D grid of targets and tuning the projection equation coefficients to get the best match between the 3-D grids projections in the image and the positions of the 3-D grids in space. Calibration parameters are stored in a file [17].

To identify the markers, the MicronTracker processes the images and matches them to the descriptors in the marker templates. Marker projections onto each image were found to always exceed a minimum footprint diameter of 9–11 pixels within the working space of our system. After identifying a marker in the image, its 3-D position is calculated by triangulating the projection rays, obtained from the calibration file, associated with the location in the image where the marker center is observed [17].

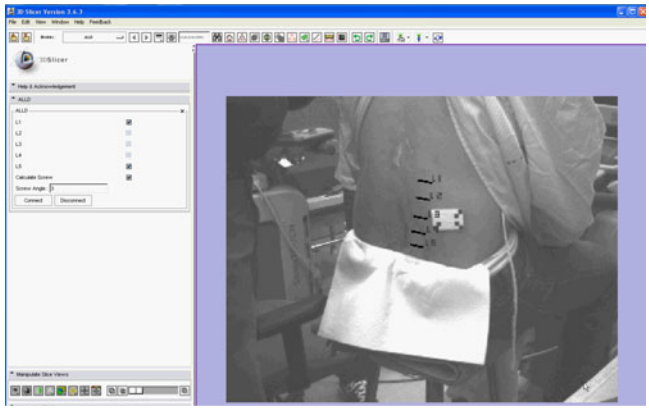

Fig. 5. Graphical user interface developed using 3-D Slicer showing the vertebral levels (black lines) overlaid on the video image of the patient's back.

We used a standard volume ray casting method [18] to overlay the identified lumbar levels on the corresponding location in a live video stream of the patient's back from the MicronTracker. A 3-D point coordinate in the camera space is transformed to a 2-D pixel location in the image plane using the MicronTracker SDK and the calibration file. To label a live video image of the patient's back, the system finds 1) the anchor transform, which is the transform between the location of the first ultrasound image and the camera and 2) the patient transform, which is the transform between the patient marker and the camera. Using the anchor and patient transforms, the system finds the transform between the anchor position of the panorama image and patient marker, which we will refer to as "Image-to-Patient" transform. Then, for each identified vertebrae, a line in the coronal plane across the vertebrae is transformed to the 3-D coordinates of the camera using the Image-to-Patient and patient marker transforms. The intersection of the projection rays with imaging plane of the MicronTracker center camera is used to calculate the location where the 3-D point will appear in the MicronTracker image and the identified lines are overlaid on the live camera view [17].

The image with the labels is transferred in real time to 3-D Slicer [19] through OpenIGTLink and displayed to the anesthesiologist on a standard monitor (see Fig. 5). Given a small range of patient motion, the positions of the overlaid lines are automatically updated as the camera tracks the changing position of the patient's marker.

III. Experiments and Results

Experiments were carried out on 17 subjects following informed consent. Ethics approval for this study was obtained from our institution's Research Ethics Board. We conducted four experiments as shown in Table I and took the following measurements:

1) Measurements on single 2-D ultrasound images:
   a) *Curvilinear vertebral height*. For each subject, the sonographer measured from the superior margin of one vertebral lamina to the superior margin of the next vertebral lamina on images obtained with a curvilinear transducer (C5-2, Ultrasonix Medical

TABLE I
TYPES OF EXPERIMENTS PERFORMED, GOLD STANDARD USED, AND MEASUREMENTS/LABELS THAT HAVE BEEN DEFINED IN THIS PAPER

Section	Experiment	Gold Standard	Measurement
A	Accuracy of vertebral height in panorama images	1a) Curvilinear vertebral height	2a) Panorama vertebral height
B	Accuracy of vertebral levels identification in panorama images	2d) Panorama vertebral levels	AREA vertebral levels
C	Accuracy of vertebral levels identification on skin	1a) Actual vertebral labels at the resting position	1d) AREA vertebral labels at the resting position
D	Accuracy after arching forward	1b) Actual vertebral labels with 5° and 10° arching forward	1e) AREA vertebral labels with 5° and 10° arching forward

Numbers used in the table refer to the measurements defined within the text.

TABLE II
MEAN (STANDARD DEVIATION) OF CURVILINEAR VERTEBRAL HEIGHT, PANORAMA VERTEBRAL HEIGHT, 90TH PERCENTILE, AND 80TH PERCENTILE OF THE ABSOLUTE ERROR CALCULATED AS THE DIFFERENCE BETWEEN THOSE TWO MEASUREMENTS

Metric	L1	L2	L3	L4	L5
Curvilinear vertebral height	31.5 (3.3)	33.4 (4.2)	33.5 (5.3)	31.8 (4.1)	31 (4)
Panorama vertebral height	28.9 (4.8)	32.9 (5)	35.1 (6)	38.2 (8.6)	35.7 (8.7)
Mean absolute error	5.4	5.5	5.8	10	8.4
90th percentile of absolute error	9.4	12.5	11.3	17.2	19.6
80th percentile of absolute error	8.2	11.1	10.3	15.5	13.9

Units are in millimetres; N=17.

Corp., Richmond, Canada). This transducer was used as it is capable of displaying two to three vertebral lamina in a single ultrasound image.

2) Measurements on the panorama image:
   a) *Panorama vertebral levels*. The sonographer identified each vertebral levels on the panorama images. She marked the midpoint of the shadow generated by the posterior surfaces of the laminae.
   b) *AREA vertebral levels.* AREA identified the vertebral levels on the panorama images.
   c) *Kerby vertebral levels.* Kerby *et al.*'s algorithm [7] was used to identify vertebral levels on the panorama images. A brief description of this algorithm is provided later.
   d) *Panorama vertebral height.* The sonographer determined the height of the vertebrae in the panorama images, by measuring from the superior margin of one vertebral lamina to the superior margin of the next lamina.
   e) *AREA vertebral count.* AREA was used to count the number of vertebrae in the panorama image.
   f) *Kerby vertebral count.* Kerby *et al.*'s algorithm was used to count the number of vertebrae in the panorama image.
3) Measurements on the skin:
   a) *Actual vertebral labels at the resting position.* These measurements were performed with each subject sitting in a comfortable upright position without purposefully arching the spine forward (i.e., sitting in the "resting" position). The sonographer used the linear array transducer to manually identify the five lumbar vertebrae either by scanning up from the sacrum or scanning down from the bottom rib and labeled the midpoint of each lumbar vertebrae on the subject's skin with a felt pen.
   b) *Actual vertebral labels with arching forward.* The measurements above were repeated while each subject arched forward until the screw angle (see Section III-D. for the description of the screw angle) of the patient marker, relative to the resting position, was changed by 5° and 10°, respectively.
   c) *Actual vertebral count*. The sonographer used the linear array transducer to manually count the five lumbar vertebrae either by scanning up from the sacrum or scanning down from the bottom rib.
   d) *AREA vertebrae labels at the resting position*. These measurements were performed with each subject sitting in the resting position. The sonographer acquired a sequence of ultrasound images, and AREA displayed virtual markings of the identified vertebral levels on an augmented video of the subject's back. The vertebral levels, which appear on the monitor, were used to label each subject's back with a felt pen.
   e) *AREA vertebrae labels with arching forward*. The measurements above were repeated while each subject arched forward until the screw angle of the patient marker, relative to the resting position, was changed by 5° and 10°, respectively.

The experiments were divided into the following parts.

A. Accuracy of Vertebral Height in Panorama Image

This experiment tested the accuracy of generating panorama images by AREA. The sonographer obtained the curvilinear vertebral height and panorama vertebral height measurements, then the absolute error was calculated between those two measurements. Measurement of vertebral height from the curvilinear probe as well as the panorama images and the difference between those two measurements are reported in Table II. In summary, two different transducers and two different scanning methods (single image versus panorama) were used in order to have two independent measurements of the vertebral height. We used the nonparametric Mann–Whitney-U test to compare

TABLE III
MEAN (STANDARD DEVIATION) AND 90TH PERCENTILE OF THE ABSOLUTE ERROR BETWEEN AREA AND PANORAMA VERTEBRAL LEVELS, AND BETWEEN KERBY AND PANORAMA VERTEBRAL LEVELS

Vertebra	L1	L2	L3	L4	L5
Mean absolute error between AREA and Panorama vertebral levels	4.2 (3)	2.5 (2.4)	3 (2.8)	3.7 (4.2)	2.7 (2.2)
Mean absolute error between Kerby and Panorama vertebral levels	2.2 (1.8)	4.4 (5.1)	4.4 (6.2)	2.9 (3.3)	2.3 (2)
90th percentile of absolute error between AREA and Panorama vertebral levels	8.6	6.4	7.2	9.1	6.4
90th percentile of absolute error between Kerby and Panorama vertebral levels	4.6	10.9	9.1	10.1	6.2

Units are millimetres, N=17.

TABLE IV
NUMBER OF FALSE AREA AND KERBY VERTEBRAL COUNTS (N = 82)

Method/Vertebra	L1	L2	L3	L4	L5
No. of false AREA vertebral levels	0	2	0	1	0
No. of false Kerby vertebral levels	0	1	0	0	0

Using the linear transducer, the sonographer could not identify three of the vertebrae because they were fused with a neighbouring vertebra.

TABLE V
ACTUAL VERTEBRAL COUNT, AREA VERTEBRAL COUNT, AND KERBY VERTEBRAL COUNT (N = 82)

Method	L1	L2	L3	L4	L5
Actual vertebral count	16	17	17	17	15
AREA vertebral count	16	16	17	16	14
Kerby vertebral count	16	15	14	15	13

For the actual vertebral count, the sonographer could not identify three of the vertebrae because they were fused with a neighbouring vertebra.

TABLE VI
MEAN (STANDARD DEVIATION), 90TH, AND 80TH PERCENTILE OF THE ABSOLUTE DIFFERENCE BETWEEN AREA ACTUAL VERTEBRAE LABELS AT THE RESTING POSITION AND ACTUAL VERTEBRAE LABELS AT THE RESTING POSITION MEASURED ON SUBJECT'S BACK

Percentile	L1	L2	L3	L4	L5
Mean	13.6 (10.9)	8.1 (7.5)	4.2 (3.5)	4.2 (4.7)	4.2 (4.5)
90th pecentile	34.6	19.7	8.8	9.7	11.6
80th percentile	19	16.2	8	7.5	9.1

Units are millimetres, N=17.

the measurements obtained with the two approaches. The test fails to show statistically significant difference between the two measurements ($p > 0.05$), except for L4 ($p = 0.005$). We also report the 90th and 80th percentile of the error for each vertebra.

B. Accuracy of Vertebral Levels Identification in Panorama Image

In order to evaluate the accuracy of AREA vertebral levels identification algorithm, we measured the distance between panorama vertebral levels and AREA vertebral levels. We also compared the performance of vertebral levels identification technique proposed in this paper with a competing method previously developed by Kerby *et al.* [7]. Error was calculated as the distances between panorama vertebral levels and Kerby vertebral levels identified in the panorama images. Kerby *et al.*'s algorithm first applies a median filter with a window width and height twice the ultrasound signal wavelength. Then, a linear filter, which operates in the vertical and horizontal directions, is used to highlight bone edges and enhance the periodic nature of the vertebrae. After that, hard thresholding is used to set two-thirds of pixels to zero, and at least squares parabolic is fit into the image. For each parabolic fit into the image, the minimum is identified as vertebra. More details can be found in the Kerby *et al.*'s paper [7].

AREA and Kerby *et al.*'s algorithms were compared in terms of the mean absolute error, number of the vertebrae identified, and the number of false identification. The results are reported in Tables III, IV, and V. The false identification reported in Table IV is mostly around the interspinous gaps because of low image intensity at that location, which occasionally results in inaccurate segmentation of the panorama image using Otsu's threshold, and subsequently, wrong identification at the interspinous gaps. The Mann–Whitney-U test comparing the absolute errors reported by AREA and Kerby *et al.*'s algorithms in Table III fails to show statistically significant difference between the two measurements ($p > 0.05$).

C. Accuracy of Vertebral Levels Identification on the Skin

To test the accuracy of identifying and overlaying vertebral levels on a live video stream of the patient's back, the error was defined as the distance between AREA actual vertebrae labels at the resting position and actual vertebrae labels at the resting position. This error was measured on the skin of the volunteer, and the mean absolute error and standard deviation of this error are reported in Table VI. We also report the 90th and 80th percentile errors for these measurements.

D. Accuracy of Spine Arching

In spinal needle insertion procedures, the patient is typically asked to arch forward to increase the width of the window to the epidural space. However, the patient may change their arch after being imaged by AREA, and change the location of vertebral levels with respect to the patient marker. After the system identifies the vertebral levels at the resting position, we asked each subject to arch further forward until the screw angle of the marker was changed by 5° and 10°, respectively. We use screw angle measurements to determine the relative

TABLE VII
COMPARISON OF THE MEAN ABSOLUTE ERROR OF AREA FOR DIFFERENT SPINE ARCHING ANGELS

Angle	L1	L2	L3	L4	L5	Total Mean absolute error
0°	13.6	8.1	4.2	4.2	4.2	6.9
5°	16.5	7.1	4.7	9.2	11.3	9.7
10°	23.7	10.5	6.3	7.9	11.7	11.9

Units are millimetres, N=17.

rotation of the marker orientation between two arching positions of the patient. All measurements are performed relative to the orientation Φ of the patient marker in the resting position of the subject and is calculated as in (2) in Spoor *et al.* [20]:

$$R = \begin{bmatrix} R_{11} & R_{12} & R_{13} \\ R_{21} & R_{22} & R_{23} \\ R_{31} & R_{32} & R_{33} \end{bmatrix} \tag{1}$$

$$\Phi = \sin^{-1}(\sqrt{(R_{32} - R_{23})^2 + (R_{13} - R_{31})^2 + (R_{21} - R_{12})^2}) \tag{2}$$

where R is the rotation matrix around the screw axis.

For each subject, the volunteer is asked to arch forward until the screw angle of the marker was changed by 5° with respect to the resting position. Then, the distance between actual vertebrae labels with 5° arching forward and AREA actual vertebrae labels with 5° arching forward was measured on the volunteer's back.

After that the volunteer is asked to arch further forward again until the screw angle of the marker was changed by 10° with respect to the resting position. Then, the distance between actual vertebrae labels with 10° arching forward and AREA actual vertebrae labels with 10° arching forward was measured on the volunteer's back. The mean absolute of these measurements for each vertebral level are reported in Table VII.

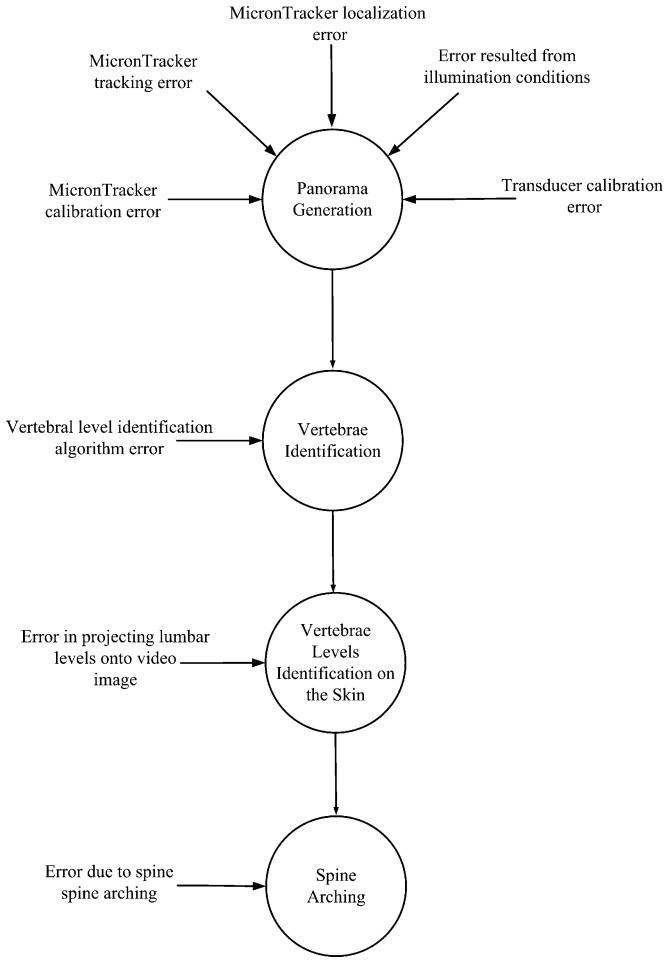

Fig. 6. Summary of major factors contributing to the overall error. Each arrow indicates an error contributing to each of the modules in the system.

IV. DISCUSSION

We presented a novel needle puncture site selection system for reducing the risk associated with lumbar spine needle insertion. The new augmented reality system concept has been successfully tested on 17 subjects, and results show the accuracy of identifying lumbar vertebral levels and overlaying the information onto a live video stream of the patient's back (mean absolute error $\simeq$21% of the vertebral height). Fig. 6 shows simple transformation chain to illustrate the major factors contributing to the total system error. In the following sections, we provide further descriptions of the various sources of the error in each step. Note that the vertebral level is considered to be identified correctly if the error is less than half the vertebral height.

A. Accuracy of Vertebrae Height in Panorama Images

In this experiment, the mean absolute error between curvilinear vertebral height and panorama vertebral height was 7.1 mm. However, this error indicates that the accuracy of generating panorama images by the proposed system is accurate enough for the purpose of vertebral levels identification (less than half the vertebral height). The major factors contributing to this error include: ultrasound image calibration error ($\simeq$ 1 mm), patient motion during the acquisition of tracked ultrasound images, acquiring images out of plane, MicronTracker localization error, and MicronTracker calibration error.

Further improvements may be possible by using a 3-D transducer and an algorithm to automatically select optimal images from each acquired ultrasound volume. This may improve the generation of the panorama images which subsequently may improve the overall system performance. Moreover, a more accurate tracking system could be used but at greater cost.

B. Accuracy of Vertebral Levels Identification in Panorama Images

We also reported the accuracy of vertebral levels identification. This experiment shows the accuracy of AREA in identifying individual vertebra in the panorama images. As shown in Tables III, IV, and V, the mean absolute error of vertebral levels identification is 3.2 mm with an identification rate of 96% and false identification rate of 3.7% (three false identifications). The false negatives are due to weak reflection from the posterior surface of the lamina in the panorama images. The false positives are mostly because of low image intensity at the interspinous gaps which result in inaccurate segmentation of the panorama image using Otsu's threshold.

In addition, AREA vertebral levels identification was compared to the Kerby *et al.*'s algorithm as shown in Table III. The mean absolute error of AREA vertebral levels identification and Kerby *et al.*'s algorithm, as well as the 90th percentile of those errors, are both less than half the vertebral height which indicates that both methods can be used to identify the levels. However, the AREA identification rate is 96% while the Kerby *et al.*'s algorithm identification rate is only 89%.

As shown in Table V, AREA identified the L3 vertebrae, the typical injection site, for all subjects while most of the Kerby *et al.*'s algorithm false identifications were for L3. The false identification rate of AREA is 3.7% (three false identifications) compared to 1.2% (one false identification) of Kerby *et al.*'s algorithm. This error is not expected to affect the outcome of needle puncture site selection since the operator can visually determine the false identification from the augmented lines on the video of the patient's back and the generated panorama image.

The vertebral levels identification error of 3.2 mm may be reduced by registering statistical shape model [21] of the lumbar spine anatomy to the panorama image which, in turn, provides more data for vertebra identification but at greater computational expense. Moreover, using a more accurate tracking system will also improve the outcome of panorama generation and vertebral levels identification modules at higher cost.

C. Accuracy of Vertebral Levels Identification on the Skin

The overall system accuracy is shown in Table VI with a total mean absolute error of 6.9 mm (shown in Table VII). As shown in Table VII, the mean absolute error is less than half the vertebral height except for L1 vertebra. This higher error for L1 is likely due to the fact that the L1 vertebra has low intensity and a flat shape in ultrasound images; thus it is difficult to define the midpoint of the shadow generated by the posterior surface of the lamina. All the previous modules contributed to the error of this stage. Specifically, this includes the errors from projecting the identified lumber levels onto a live video of the patient's back.

D. Accuracy of Spine Arching

In the arching accuracy experiment, given forward arching of the subject up to 10°, the maximum mean absolute error observed was 11.9 mm. Given that the marker was affixed to the patient's back close to L3, the error was highest for the vertebrae farthest away, i.e., L1 and L5. The mean absolute error increases with forward arching due to the increase of the distance away from the patient marker. These errors are less significant because L1 and L5 are farthest from the typical injection site that is generally close to L3 (L3-L4 or L2-L3). If needed, the error of L1 and L5 could be also reduced by using multiple tracking markers on the skin of the patient that span the sacral, lumbar, and thoracic region.

The proposed system introduces less than 2 min overhead to the routine clinical examination process. This includes acquiring tracked ultrasound images, vertebral levels identification, and overlaying the identified levels on a live video image of the patient's back. One drawback of this system is the fact that missing vertebra will result in wrong labeling of the vertebrae of the levels. Therefore, the system allows the operator to decide the first and last vertebrae to be imaged and thereafter used to count, label, overlay, and display those labels. In the future, the system can be further developed to allow the operator to specify the missing vertebral labels which will help in case there is any missing vertebra other than L5 and L1.

Another possible drawback is the increase in intervening tissue in obese patients between the ultrasound probe and lamina which may affect the image quality and results of lumbar identification. However, using the AREA vertebral levels identification algorithm, in which segmentation and vertebrae identification parameters are automatically chosen depending on the properties of the panorama image, will have a minor effect on the results compared to Kerby *et al.*'s algorithm which use simple threshold by zeroing two-thirds of the pixels. More tests on obese patients are needed.

The performance of the panorama generation step will degrade in the presence of large transducer rotations. To analyze the effect of such rotations, we performed an experiment where we scanned a volunteer ten times from L5-S1 to T12-L1, and successfully generated ten independent panorama images. We measured the rotation of the scan planes relative to the first scan plane in each generated panorama image. The extent of rotation around the axial axis is $4.1^\circ \pm 5^\circ$, the extent of rotation around the lateral axis is $0.9^\circ \pm 7.7^\circ$, and the extent of rotation around the elevation axis is $9.5^\circ \pm 10.2^\circ$. These rotation angles indicate the range of probe rotations during panorama acquisition, while anatomically correct features are visible in the acquired ultrasound scans. We would like to emphasize that the acceptable range is most likely operator and subject specific.

In conclusion, AREA provides an objective and consistent measure for the identification of the vertebral levels based on the panorama image depicting the entire lumbar region, as opposed to local vertebral identification using single ultrasound image acquisitions at each level. Also, the method provides an overlay of the plan onto the patient's back, therefore minimizing the procedure variability due to the interpretation of the sonographer. The accuracy of AREA is within the clinically acceptable range, which is less than half the vertebral height, for L3 vertebra where most needle insertions are performed. This system is designed to fit within the established clinical workflow for epidural anesthesia. It could be used prior to performing the needle insertion procedure without the requirement for special patient preparation. Moreover, AREA is intended to be used by a single operator without disrupting the sterile field since the only computer interaction is via a foot pedal. This proof of concept therefore is the first step before subsequent testing in clinical practice.

ACKNOWLEDGMENTS

This work is jointly funded by grants from the Natural Sciences and Engineering Research Council of Canada and the Canadian Institutes of Health Research.

REFERENCES

[1] S. Liu, W. Strodtbeck, J. Richman, and C. Wu, "A comparison of regional versus general anesthesia for ambulatory anesthesia: A meta-analysis of randomized controlled trials," *Anesthesia Analgesia*, vol. 101, pp. 1634–16342, Dec. 2005.

[2] F. Reynolds, "Logic in the safe practice of spinal anaesthesia," *Anaesthesia*, vol. 55, pp. 1045–1046, Nov. 2000.

[3] G. Furness, M. Reilly, and S. Kuchi, "An evaluation of ultrasound imaging for identification of lumbar intervertebral level," *Anaesthesia*, vol. 57, pp. 277–280, Mar. 2002.

[4] H. Schlotterbeck, R. Schaeffer, W. Dow, Y. Touret, S. Bailey, and P. Diemunsch, "Ultrasonographic control of the puncture level for lumbar neuraxial block in obstetric anaesthesia," *Brit. J. Anaesthesia*, vol. 100, pp. 230–234, Feb. 2008.

[5] M. Yamauchi, E. Honma, M. Mimura, H. Yamamoto, E. Takahashi, and A. Namiki, "Identification of the lumbar intervertebral level using ultrasound imaging in a post-laminectomy patient," *J. Anesthesia*, vol. 20, pp. 231–233, Aug. 2006.

[6] A. Rasoulian, J. Lohser, M. Najafi, H. Rafii-Tari, D. Tran, A. Kamani, V. Lessoway, P. Abolmaesumi, and R. Rohling, "Utility of prepuncture ultrasound for localization of the thoracic epidural space," *Can. J. Anesthesia J. Can. d'Anesthésie*, vol. 58, pp. 1–9, Sep. 2011.

[7] B. Kerby, R. Rohling, V. Nair, and P. Abolmaesumi, "Automatic identification of lumbar level with ultrasound," in *Proc. Eng. Med. Biol. Conf.*, Vancouver, BC, Canada, Aug. 2008, pp. 2980–2983.

[8] H. Rafii-Tari, "Panorama ultrasound for navigation and guidance of epidural anesthesia" Master's thesis, Univ. British Columbia, BC, Canada, 2011.

[9] H. Ashab, V. Lessoway, S. Khallaghi, A. Cheng, R. Rohling, and P. Abolmaesumi, "Area: An augmented reality for epidural anaesthesia," in *Proc. Eng. Med. Biol. Conf.*, San Diego, CA, USA, Aug. 2012, pp. 2659–2663.

[10] A. Lasso, T. Heffter, C. Pinter, T. Ungi, T. K. Chen, A. Boucharin, and G. Fichtinger, "Plus: An open-source toolkit for developing ultrasound-guided intervention systems," in *Proc. 4th NCIGT NIH Image Guided Therapy Workshop*, Oct. 2011, vol. 4, p. 103.

[11] L. Ibanez, W. Schroeder, L. Ng, and J. Cates *The ITK software guide: The insight segmentation and registration toolkit*, Kitware, Inc., NY, USA, vol. 5, 2003.

[12] L. Maier-Hein, A. Franz, H. Meinzer, and I. Wolf, "Comparative assessment of optical tracking systems for soft tissue navigation with fiducial needles," in *Proc. Med. Imag.: Vis. Imag. Guided Procedures Model.*, San Diego, CA, USA, Mar. 2008, pp. 69181Z-1–69181Z-9.

[13] C. Tomasi and R. Manduchi, "Bilateral filtering for gray and color images," in *Proc. 6th Intell. Conf. Comput. Vis.*, Bombay, India, Jan. 1998, pp. 839–846.

[14] I. Hacihaliloglu, R. Abugharbieh, A. Hodgson, and R. Rohling, "Bone surface localization in ultrasound using image phase-based features," *Ultrasound Med. Biol.*, vol. 35, pp. 1475–1487, Sep. 2009.

[15] A. Jain and R. Taylor, "Understanding bone responses in B-mode ultrasound images and automatic bone surface extraction using a bayesian probabilistic framework," in *Proc. SPIE Med. Imag.*, Bellingham, WA, USA, Apr. 2004, pp. 131–142.

[16] N. Otsu, "A threshold selection method from gray-level histograms," *IEEE Trans. Syst. Man Cybern.*, vol. 9, no. 1, pp. 62–66, Jan. 1979.

[17] *Microntracker developers manual MTC 3.6*, Claron Technology, Inc., Toronto, ON, Canada, 2008.

[18] J. Udupa and G. Herman, *3D Imaging in Medicine*. Boca Raton, FL, USA: CRC Press, 1999.

[19] D. Gering, A. Nabavi, R. Kikinis, W. Grimson, N. Hata, P. Everett, F. Jolesz, and W. Wells, "An integrated visualization system for surgical planning and guidance using image fusion and interventional imaging," in *Proc. 2nd Int. Med. Imag. Comput. Comput.-Assist. Intervent.*, Sep. 1999, vol. 1679, pp. 809–819.

[20] C. Spoor *et al.*, "Rigid body motion calculated from spatial co-ordinates of markers," *J. Biomech.*, vol. 13, pp. 391–393, Feb. 1980.

[21] A. Rasoulian, R. Rohling, and P. Abolmaesumi, "Group-wise registration of point sets for statistical shape models," *IEEE Trans. Med. Imag.*, vol. 31, no. 11, pp. 2025–2034, Nov. 2012.

Authors', photographs and biographies not available at the time of publication.